

Multifaceted impact of a surface step on superconductivity in atomically thin films

L.-F. Zhang,¹ L. Flammia,^{1,2} L. Covaci,¹ A. Perali,³ and M. V. Milošević^{1,*}

¹*Departement Fysica, Universiteit Antwerpen, Groenenborgerlaan 171, B-2020 Antwerpen, Belgium*

²*School of Science and Technology, Physics Division, University of Camerino, 62032 Camerino, Italy*

³*School of Pharmacy, Physics Unit, University of Camerino, 62032 Camerino, Italy*

Recent experiments show that an atomic step on the surface of atomically thin metallic films can strongly affect electronic transport. Here we reveal multiple and versatile effects that such a surface step can have on superconductivity in ultrathin films. By solving the Bogoliubov-de Gennes equations self-consistently in this regime, where quantum confinement dominates the emergent physics, we show that the electronic structure is profoundly modified on the two sides of the step, as is the spatial distribution of the superconducting order parameter and its dependence on temperature and electronic gating. Furthermore, the surface step changes non-trivially the transport properties both in the proximity-induced superconducting order parameter and the Josephson effect, depending on the step height. These results offer a new route to tailor superconducting circuits and design atomically thin hetero-junctions made of one same material.

PACS numbers: 74.78.-w, 74.20.Pq, 74.81.-g

Over the last decade, atomically thin films were found to exhibit rich superconducting phenomena, often not achievable in their bulk counterparts [1–4]. This field of research was opened by discovery that Pb, In and Ga films can retain superconductivity down to thickness of few atomic monolayers [5–9], in spite of expected detrimental effects of thermal and/or quantum fluctuations [10, 11]. More recent discoveries include a strong enhancement of critical temperature T_c in the one-unit cell thick FeSe films on SrTiO₃, above 100 K compared to 8 K of the bulk FeSe [12]; the monolayers of NbSe₂ exhibit spin-momentum locking effect leading to a very high in-plane critical magnetic field [13]; the monolayer TI-Pb compound hosts giant Rashba spin-split states, potentially useful for superconducting spintronics. In all such crystalline and atomically thin materials superconductivity is known to be strongly affected by quantum confinement, leading to observable thickness-dependent quantum size effects [5, 14–21] and distinctly different electronic properties. Understanding and controlling these is the key to engineering electronic devices with novel functionalities.

Recently, a step on the surface of atomically thin films, even if just one atom high, was found to strongly influence the electronic transport. Such surface steps not only change the overall electronic structure of the film, but also affect the range of proximity-induced superconducting correlations and the interplay of superconducting currents. Refs. [22, 23] have demonstrated that an atomic surface step disrupts superconductivity, blocks supercurrents, pins Josephson vortices, and works as an intrinsic Josephson junction. Furthermore, the surface step was recently found to terminate the propagation of the proximity-induced superconducting pair correlation [24]. Therefore, engineering the atomic steps on the surface of crystalline films is a definite new route to optimize and manipulate the superconducting properties or device per-

formance at and below nanoscale.

In this Letter, we show that above-mentioned effects are only some particular examples, as a surface step actually exhibits a multifaceted influence on the electronic, superconducting and transport properties of atomically thin films. Due to the interplay between the quantum confinement effects and the scattering induced by the surface step, we find that physical properties on two sides of the step can be qualitatively and quantitatively different for both normal and superconducting state of the film. In addition, the transport is also affected by quantum resonances related to film thickness, with performance characteristics tunable by the height of the step on the surface. Our findings not only improve the understanding of the role of surface steps in superconductivity but also facilitate the further design of atomic-scale superconducting quantum devices.

We employ the Bogoliubov-de Gennes (BdG) equations in this study, proven effective in the past to detect and understand the interplay between superconducting phase and the quantum confinement effect in nanoscale samples [14, 15, 25–27]. The BdG equations are written as:

$$[K_0 - E_F] u_n(\vec{r}) + \Delta(\vec{r}) v_n(\vec{r}) = E_n u_n(\vec{r}), \quad (1)$$

$$\Delta(\vec{r})^* u_n(\vec{r}) - [K_0^* - E_F] v_n(\vec{r}) = E_n v_n(\vec{r}), \quad (2)$$

where $K_0 = -(\hbar\nabla)^2/2m + U(\vec{r})$ is the kinetic energy with U being the one-particle potential and E_F the Fermi energy, $u_n(v_n)$ are electron(hole)-like quasiparticle eigen-wavefunctions, and E_n are the quasiparticle eigen-energies. The pair potential $\Delta(\vec{r})$ is determined self-consistently from the eigen-wavefunctions and eigen-energies as:

$$\Delta(\vec{r}) = g \sum_{E_n < E_c} u_n(\vec{r}) v_n^*(\vec{r}) [1 - 2f(E_n)], \quad (3)$$

where g is the coupling constant, E_c the Debye cutoff

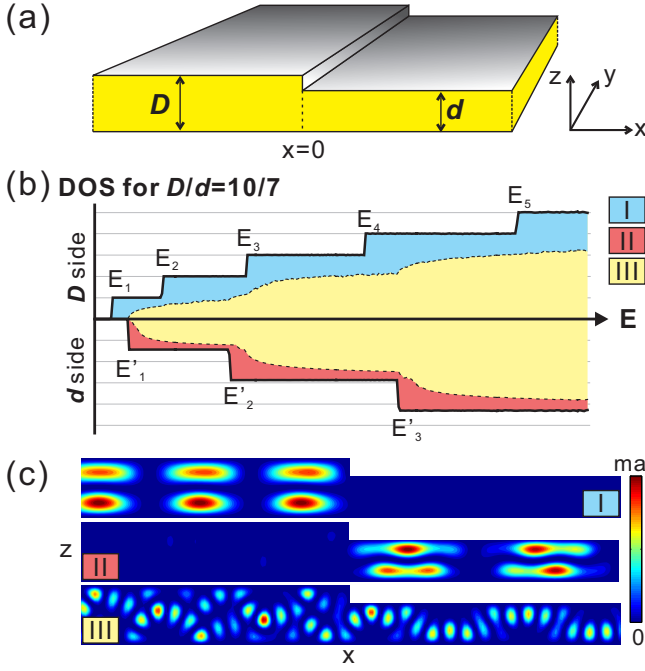


FIG. 1. (Color online) (a) The oblique view of a film with surface step. The thicknesses of two sides of the step are labelled D and d . The lateral dimensions of the film are taken large enough in the simulations and do not affect the presented results. (b) Normal-state electronic structure for $D/d = 10/7$. The top panel shows the spatial average of LDOS on two sides of the step. The color coding indicates the three classes of states (denoted I-III) and their portion in the total density. (c) The electronic probability density distributions for typical states I-III.

energy, and $f(E_n) = [1 + \exp(E_n/k_B T)]^{-1}$ the Fermi distribution function, where T is the temperature.

We consider a laterally extended film with a surface step, schematically depicted in Fig. 1(a). The thicknesses of the left and right side of the step are labelled D and d , respectively. We require that the wavefunctions $u_n(\vec{r})$ and $v_n(\vec{r})$ decay exponentially in the vacuum outside the film, by setting the potential to a large value, $U(\vec{r}) = 20E_F$. Under this condition, we solve the BdG equations (1)-(3) self-consistently by expanding u_n and v_n in term of Fourier series [28]. Since there exist by now a large variety of ultrathin superconducting structures, e.g. made of Pb, In, Ga, NbSe₂, we chose to keep the calculations generic and not include the specific band-structure of either material. Instead, we considered an isotropic quadratic dispersion and confirmed that the shown features remain robust for a wide range of parameters, i.e. $k_F \xi_0 \approx 20 - 200$, where k_F is the Fermi wave vector, ξ_0 and Δ_0 are the coherence length and the bulk superconducting gap at $T = 0$, respectively. Thus, without loss of generality, we set the parameters to: effective mass $m = 1.5m_e$ (m_e is the electron mass), $k_F \xi_0 = 2E_F/\Delta_0 \approx 100$ and $E_c/\Delta_0 \approx 10$.

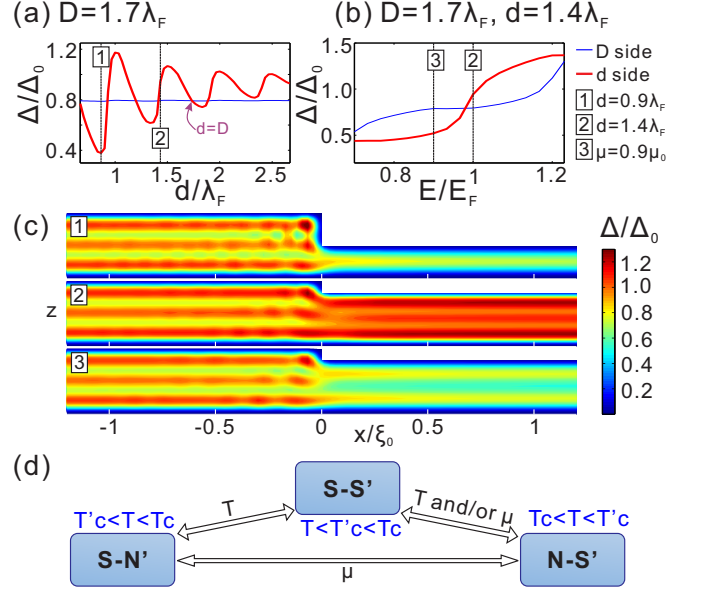


FIG. 2. (Color online) Superconducting properties. Panel (a) shows the spatial average of $|\Delta(x, z)|$ over two sides of the step, as a function of d for $D = 1.7\lambda_F$. Panel (b) shows the same but as a function of E for $D = 1.7\lambda_F$ and $d = 1.4\lambda_F$. (c) The spatial profiles of the order parameter for the selected cases 1-3. (d) The chart for tuning the system into $S-S'$, $S-N'$ and $N-S'$ junctions by changing temperature T and/or chemical potential μ .

Since any effect of the surface step on electron wave functions may further manifest in the superconducting order parameter, we first examine the normal-state electronic structure - well characterized by the spatial average of the LDOS (DOS) over D and d sides of the step. As an exemplary case, Fig. 1(b) shows the DOS of both sides for $D/d = 10/7$. The film exhibits the standard 2D DOS of quantum wells on either side of the surface step, but with different characteristic energies, i.e. a staircase in DOS is observed at energies $E_j = \hbar^2(\pi j/D)^2/2m^*$ and $E'_j = \hbar^2(\pi j'/d)^2/2m^*$ on respective sides of the step. To understand the consequences of the latter, we examine also the normal state wavefunctions. We find that the resulting normal states can be grouped into three classes [exemplified in Fig. 1(b)]: with probability density concentrated on thicker side (class I), on thinner side (II), or densities mixed across the step (III).

The states of class I (II) are similar to the quantum-well states. They emerge abruptly at threshold energies E_j (E'_j), and are responsible for the staircase rise of DOS [c.f. the color coding in DOS in Fig. 1(b)]. As a result, the electronic properties on one side of the step on the surface can be very different from those on the other, especially when the Fermi energy is close to E_j or E'_j . At higher energy, the states of class I and II increasingly mix, and states of class III dominate the DOS. Therefore the difference in DOS at the surface step becomes negligi-

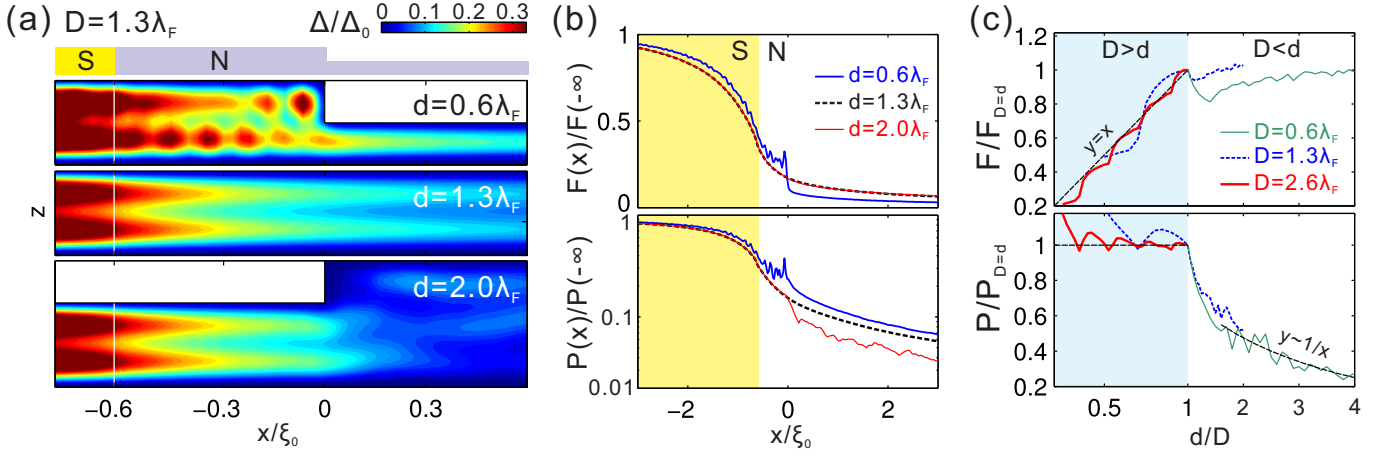


FIG. 3. (Color online) The effect of a surface step on the proximity-induced superconducting order parameter (OP). (a) The spatial OP profile near the surface step for $d/\lambda_F = 0.6, 1.3$ and 2 , for fixed $D = 1.3\lambda_F$. The S-N interface is located at $x = -0.6\xi_0$, as depicted in the top cartoon. (b) $F(x)$, the total OP (integrated over z), and $P(x)$, the maximum of the OP over z , as a function of x for the three cases shown in panel (a). (c) $F/F_{D=d}$ and $P/P_{D=D}$ at $x = \xi_0$ as a function of d/D for $D/\lambda_F = 0.6, 1.3$, and 2.6 . The shaded area highlights the different behavior for $d < D$ compared to $d > D$ case.

ble for $j, j' \rightarrow \infty$, and homogeneous electronic properties in the film are recovered. In other words, the surface step is particularly important for atomically thin films, and the peculiar electronic structure in that case is the consequence of the interplay between different quantum confinement effect on two sides of the step and the electron scattering at the surface step.

After understanding fundamental normal state properties of the system, we turn to the analysis of the superconducting state. We first calculated the spatial average of the superconducting order parameter on two sides of the step, namely $\bar{\Delta}_D$ and $\bar{\Delta}_d$. Fig. 2(a) plots those quantities as a function of d for fixed $D = 1.7\lambda_F$, and reveals that $\bar{\Delta}_D$ does not change with d while $\bar{\Delta}_d$ exhibits d -dependent oscillations due to quantum size effect. As a consequence, $|\Delta|$ on one side of the step on the surface can be very different from that on the other side, depending on the thicknesses D and d (relatively easily realized between 2 and 20 monolayers for e.g. Pb [6]). For example, for $D = 1.7\lambda_F$, $|\Delta|$ in the D side is higher than on the other side when $d = 0.9\lambda_F$, while situation is reversed for $d = 1.4\lambda_F$ [see cases 1 and 2 marked in Fig. 2(a)].

The order parameter is not only sensitive to thickness D and d , but can also be broadly tuned by the shift of Fermi energy E_F , via e.g. electronic gating[29]. Fig. 2(b) shows the evolution of $\bar{\Delta}_D$ and $\bar{\Delta}_d$ with varied E_F , for $D = 1.7\lambda_F$ and $d = 1.4\lambda_F$. As seen, $\bar{\Delta}_D$ and $\bar{\Delta}_d$ alternately dominate each other with changing E_F , as a consequence of normal state DOS being the staircase functions. Compared to the case 2 at $E = E_F$ where $\bar{\Delta}_D < \bar{\Delta}_d$, in the case 3 at $E = 0.9E_F$ we realize $\bar{\Delta}_D > \bar{\Delta}_d$. This feature is clearly seen in the contour plots of $|\Delta(x, y)|$ in Fig. 2(c) for the three selected cases. One should notice

in these plots additional oscillations of the order parameter near the surface step due to non-negligible scattering.

Employing the above features, one can realize S-S', S-N' and N-S' (S, S' superconductor, N, N' normal metal) junctions in one same film with atomically defined step in thickness, nearly at will. In Fig. 2(d) we provide a schematic diagram for such tuning, done by changing chemical potential and/or temperature. Due to different Andreev reflection and proximity effect in these three types of junctions, different electrical conductance can be realized, or used in thermal or electronic sensors. Additional functionalities of the device can be achieved in case of two (or more) steps on the film surface, in close proximity to each other.

To reveal more facets of the influence of surface step on superconductivity in ultrathin films, we studied transport properties in the system. Motivated by the recent experiment of Ref. [24], we present in Fig. 3 how the proximity-induced order parameter changes when crossing the step in thickness. In the considered case the step itself is in the normal state, and superconducting correlations originate from distance $0.6\xi_0$ away from the step. We find that superconducting transport from thick film into thin film ($D > d$) strongly differs from the opposite case ($D < d$), due to different scattering induced by the surface step. Fig. 3(a) shows comparatively the contourplots of order parameter near the step for cases $D > d$, $D = d$, and $D < d$. The normal state region is at $x > -0.6\xi_0$, and order parameter (OP) is expected to decay with x . However, when $D > d$, the OP is locally enhanced by reflection from the surface step, and exhibits pronounced oscillations in the film between the S-N interface and the surface step - notably different from the case $D = d$. Surprisingly, the OP beyond the

surface step ($x > 0$) is also enhanced compared to the $D = d$ case. This is different from the observations in Ref. [24], where the surface step terminated the propagation of the proximity-induced OP. On the other hand, for $D < d$, the OP seems to decrease strongly beyond the surface step. To visualize these features more clearly, we plot in Fig. 3(b) the OP integrated over the thickness [$F(x) = \int \Delta(x, z) dz$] as well as the maximal local value of $\Delta(x, z)$ [$P(x)$] for each x , for the three cases considered in Fig. 3(a). We find that $F(x)$ is abruptly suppressed when crossing the surface step for $D > d$ whereas it does not change for $D < d$, compared to the case of $D = d$. The behavior of $P(x)$ is opposite from $F(x)$ as seen also in Fig. 3(a), where $P(x)$ is enhanced when crossing the surface step for $D > d$ whereas it is suppressed for $D < d$, compared to the case of $D = d$. Note that oscillations in $F(x)$ and $P(x)$ are not due to the numerical accuracy but appear due to scattering at the interface and are pronounced in the thicker part of the sample.

In Fig. 3(c) we plot $F(x)$ and $P(x)$ at $x = \xi_0$ as a function of d , for different chosen D , in order to devise the universal rule with respect to the role of the surface step. When $d < D$, the step blocks the propagation of the Cooper pairs and $F(x = \xi_0)$ increases linearly as $d \rightarrow D$. When $d > D$, the surface step does not block the propagation and $F(\xi_0)$ weakly increases with d until saturation for $d \gg \xi_0$. $F(\xi_0)$ still shows thickness-dependent oscillatory quantized behavior, especially for $d < D$. Due to quantum confinement, the local OP density [$P(\xi_0)$] can be in resonant situation and thus enhanced for some d when $d > D$. When $d > D$, $P(x)$ on d side is always proportional to $1/d$ so OP density decreases fast when crossing the step on the film.

Our results show that the effect of the surface step on the proximity-induced OP is more diverse than the bare termination observed by STM in Ref. [24]. The latter pertinent observation is suggestive of additional scattering at the experimentally realized surface step compared to our considerations. We therefore introduce an additional potential barrier at the surface step [shown in Fig. 4(a)], because the surface step breaks the lattice translation symmetry, which can significantly modify the electronic structure and shift the chemical potential. Such a potential barrier always has a detrimental effect on the proximity-induced OP at the surface step. However, in that case we have additional new physics stemming from the fact that potential barrier at the step can be considered as a weak link. To capture those effects, we study DC Josephson tunneling by imposing a phase difference θ between the two sides of the step on the surface [30]. In practice, we set $\Delta(x < -\xi_0) = |\Delta|$ and $\Delta(x > \xi_0) = |\Delta|e^{i\theta}$ on the weak link of width $2\xi_0$ where additional potential is applied [see Fig. 4(a)]. Then, the

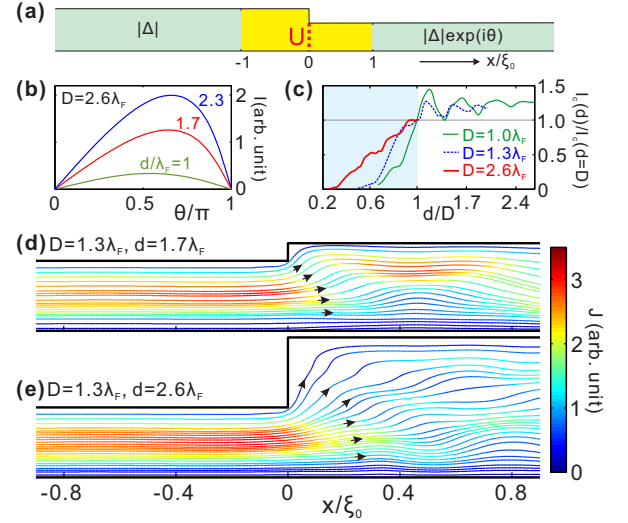


FIG. 4. (Color online) (a) Schematic picture of a Josephson junction in an ultrathin film with a step, with additional potential barrier U . (b) The current-phase relation for $D = 2.6\lambda_F$ and $d/\lambda_F = 1, 1.7$ and 2.3 . (c) Critical current I_c as a function of d/D (scaled to I_c for $d = D$), for $D/\lambda_F = 1, 1.3$, and 2.6 . The shading highlights the very different behavior observed for $d < D$ versus the case of $d > D$. (d) and (e) show the supercurrent flow through the junction for $d/\lambda_F = 1.7$ and 2.6 , respectively, for $D = 1.3\lambda_F$.

resulting supercurrent density is calculated as:

$$\vec{J}(\vec{r}) = \frac{e\hbar}{2mi} \sum_{E_n < E_c} \{ f(E_n) u_n^*(\vec{r}) \nabla u_n(\vec{r}) + [(1 - f(E_n)) v_n(\vec{r}) \nabla v_n^*(\vec{r}) - h.c.] \}.$$

The potential barrier is chosen so that we can always find the critical Josephson current I_c for $0 < \theta < \pi$, as seen from the $I - \theta$ relation in Fig. 4(b). Fig. 4(c) summarizes the effect of the surface step on the Josephson effect, where I_c was plotted as a function of d for different D . Similarly to the proximity-induced OP, the effect on Josephson current is profoundly different for $d < D$ and $d > D$. For $d < D$, I_c increases nearly linearly with d . For $d > D$, I_c oscillates with d due to quantum-size effect, until convergence. These oscillations in I_c indicate significant change in tunneling between two sides of the step. Figs. 4(d) and (e) show the streamlines of the supercurrent inside the junction. Both cases exhibit very inhomogeneous flow of current, due to quantum confinement. In Fig. 4(d), the main current channel shifts from the center/bottom of the film to the top when passing the step on surface. In contrast, Fig. 4(e) shows the case where main current channel remains in the bottom half of the film before and beyond the step. For that reason, the latter case exhibits facilitated tunneling, leading to higher critical current. This is yet another example of a useful property in superconducting devices that can be tuned to very different regimes by atomically small steps

in ultrathin films.

In summary, we showed that surface steps in atomically thin films can lead to a multitude of pronounced and diverse effects on superconductivity and transport properties. Even if small, such steps strongly modify the effects of quantum confinement in ultrathin films, while also causing significant electronic scattering. We reveal how the subtle interplay of those is tuned by the thickness, temperature, and/or electronic gating, that enables engineering of S-S', S-N' and N-S junctions at the step, nearly at will. The transport properties and the proximity-induced superconducting order parameter also exhibit versatile possible behavior (even opposite regimes) depending on the thickness of the film and the step. The needed crystalline thin films are readily fabricated experimentally, typically as laterally interconnected atomically flat islands of different thickness, and can be grown on terraced or pre-patterned substrates. The presented results are directly relevant to STM measurements near a step surface, and to the core size and other fine properties of Abrikosov vortices on either side of the step. Our findings thus open an explorable new route to superconducting quantum devices and circuitry made of one same material but with functionality locally and broadly crafted by 3D atomistic engineering and quantum effects.

This work was supported by the Research Foundation-Flanders (FWO-Vlaanderen) and the Special Research Funds of the University of Antwerp (TOPBOF project).

* milorad.milosevic@uantwerpen.be

- [1] Lili Wang, Xucun Ma, and Qi-Kun Xue, "Interface high-temperature superconductivity," *Supercond. Sci. Technol.* **29**, 123001 (2016).
- [2] Takashi Uchihashi, "Two-dimensional superconductors with atomic-scale thickness," *Supercond. Sci. Technol.* **30**, 013002 (2016).
- [3] Chuan Xu, Libin Wang, Zhibo Liu, Long Chen, Jingkun Guo, Ning Kang, Xiu-Liang Ma, Hui-Ming Cheng, and Wencai Ren, "Large-area high-quality 2D ultrathin Mo₂C superconducting crystals," *Nat. Mater.* **14**, 1135–1141 (2015).
- [4] Yu Saito, Tsutomu Nojima, and Yoshihiro Iwasa, "Highly crystalline 2D superconductors," *Nature Reviews Materials* **2**, 16094 (2016).
- [5] Yang Guo, Yan-Feng Zhang, Xin-Yu Bao, Tie-Zhu Han, Zhe Tang, Li-Xin Zhang, Wen-Guang Zhu, E. G. Wang, Qian Niu, Z. Q. Qiu, Jin-Feng Jia, Zhong-Xian Zhao, and Qi-Kun Xue, "Superconductivity Modulated by Quantum Size Effects," *Science* **306**, 1915–1917 (2004).
- [6] Mustafa M. Özer, James R. Thompson, and Hanno H. Weitering, "Hard superconductivity of a soft metal in the quantum regime," *Nat. Phys.* **2**, 173–176 (2006).
- [7] Tong Zhang, Peng Cheng, Wen-Juan Li, Yu-Jie Sun, Guang Wang, Xie-Gang Zhu, Ke He, Lili Wang, Xucun Ma, Xi Chen, Yayu Wang, Ying Liu, Hai-Qing Lin, Jin-Feng Jia, and Qi-Kun Xue, "Superconductivity in one-atomic-layer metal films grown on Si(111)," *Nat. Phys.* **6**, 104–108 (2010).
- [8] Agnieszka Stepniak, Augusto Leon Vanegas, Michael Caminale, Hirofumi Oka, Dirk Sander, and Jürgen Kirschner, "Atomic layer superconductivity," *Surf. Interface Anal.* **46**, 1262–1267 (2014).
- [9] Hui-Min Zhang, Yi Sun, Wei Li, Jun-Ping Peng, Can-Li Song, Ying Xing, Qinghua Zhang, Jiaqi Guan, Zhi Li, Yanfei Zhao, Shuaihua Ji, Lili Wang, Ke He, Xi Chen, Lin Gu, Langsheng Ling, Mingliang Tian, Lian Li, X. C. Xie, Jianping Liu, Hui Yang, Qi-Kun Xue, Jian Wang, and Xucun Ma, "Detection of a Superconducting Phase in a Two-Atom Layer of Hexagonal Ga Film Grown on Semiconducting GaN(0001)," *Phys. Rev. Lett.* **114**, 107003 (2015).
- [10] Allen M. Goldman and Nina Marković, "Superconductor–Insulator Transitions in the Two-Dimensional Limit," *Phys. Today* **51**, 39–44 (2008).
- [11] Yonatan Dubi, Yigal Meir, and Yshai Avishai, "Nature of the superconductor–insulator transition in disordered superconductors," *Nature* **449**, 876–880 (2007).
- [12] Jian-Feng Ge, Zhi-Long Liu, Canhua Liu, Chun-Lei Gao, Dong Qian, Qi-Kun Xue, Ying Liu, and Jin-Feng Jia, "Superconductivity above 100 K in single-layer FeSe films on doped SrTiO₃," *Nat. Mater.* **14**, 285–289 (2015).
- [13] Xiaoxiang Xi, Zefang Wang, Weiwei Zhao, Ju-Hyun Park, Kam Tuen Law, Helmuth Berger, László Forró, Jie Shan, and Kin Fai Mak, "Ising pairing in superconducting NbSe₂ atomic layers," *Nat. Phys.* **12**, 139–143 (2016).
- [14] A. A. Shanenko, M. D. Croitoru, M. Zgirski, F. M. Peeters, and K. Arutyunov, "Size-dependent enhancement of superconductivity in Al and Sn nanowires: Shape-resonance effect," *Phys. Rev. B* **74**, 052502 (2006).
- [15] M. D. Croitoru, A. A. Shanenko, and F. M. Peeters, "Dependence of superconducting properties on the size and shape of a nanoscale superconductor: From nanowire to film," *Phys. Rev. B* **76**, 024511 (2007).
- [16] Aurelio Romero-Bermúdez and Antonio M. García-García, "Shape resonances and shell effects in thin-film multiband superconductors," *Phys. Rev. B* **89**, 024510 (2014).
- [17] Aurelio Romero-Bermúdez and Antonio M. García-García, "Size effects in superconducting thin films coupled to a substrate," *Phys. Rev. B* **89**, 064508 (2014).
- [18] Y. Chen, A. A. Shanenko, A. Perali, and F. M. Peeters, "Superconducting nanofilms: molecule-like pairing induced by quantum confinement," *J. Phys.: Condens. Matter* **24**, 185701 (2012).
- [19] A. Bianconi, D. Innocenti, A. Valletta, and A. Perali, "Shape Resonances in superconducting gaps in a 2DEG at oxide-oxide interface," *J. Phys.: Conf. Ser.* **529**, 012007 (2014).
- [20] Davide Innocenti, Nicola Poccia, Alessandro Ricci, Antonio Valletta, Sergio Caprara, Andrea Perali, and Antonio Bianconi, "Resonant and crossover phenomena in a multiband superconductor: Tuning the chemical potential near a band edge," *Phys. Rev. B* **82**, 184528 (2010).
- [21] Mauro M. Doria, M. Cariglia, and A. Perali, "Multi-gap superconductivity and barrier-driven resonances in superconducting nanofilms with an inner potential barrier," *Phys. Rev. B* **94**, 224513 (2016).
- [22] C. Brun, T. Cren, V. Cherkez, F. Debontridder, S. Pons,

- D. Fokin, M. C. Tringides, S. Bozhko, L. B. Ioffe, B. L. Altshuler, and D. Roditchev, “Remarkable Effects of Disorder on Superconductivity of Single Atomic Layers of Lead on Silicon,” *Nat. Phys.* **10**, 444–450 (2014).
- [23] Shunsuke Yoshizawa, Howon Kim, Takuto Kawakami, Yuki Nagai, Tomonobu Nakayama, Xiao Hu, Yukio Hasegawa, and Takashi Uchihashi, “Imaging Josephson Vortices on the Surface Superconductor Si(111)-($\sqrt{7} \times \sqrt{3}$)-In using a Scanning Tunneling Microscope,” *Phys. Rev. Lett.* **113**, 247004 (2014).
- [24] Howon Kim, Shi-Zeng Lin, Matthias J. Graf, Yoshinori Miyata, Yuki Nagai, Takeo Kato, and Yukio Hasegawa, “Electrical Conductivity through a Single Atomic Step Measured with the Proximity-Induced Superconducting Pair Correlation,” *Phys. Rev. Lett.* **117**, 116802 (2016).
- [25] L.-F. Zhang, L. Covaci, M. V. Milošević, G. R. Berdiy-
orov, and F. M. Peeters, “Unconventional Vortex States in Nanoscale Superconductors Due to Shape-Induced Resonances in the Inhomogeneous Cooper-pair Condensate,” *Phys. Rev. Lett.* **109**, 107001 (2012).
- [26] L.-F. Zhang, L. Covaci, and F. M. Peeters, “Tomasch effect in nanoscale superconductors,” *Phys. Rev. B* **91**, 024508 (2015).
- [27] A. A. Shanenko, M. D. Croitoru, R. G. Mints, and F. M. Peeters, “New Andreev-Type States in Superconducting Nanowires,” *Phys. Rev. Lett.* **99**, 067007 (2007).
- [28] L.-F. Zhang, L. Covaci, and F. M. Peeters, “Position-dependent effect of non-magnetic impurities on superconducting properties of nanowires,” *Europhys. Lett.* **109**, 17010 (2015).
- [29] D. Daghero, F. Paolucci, A. Sola, M. Tortello, G. A. Ummarino, M. Agosto, R. S. Gonnelli, Jijeesh R. Nair, and C. Gerbaldi, “Large Conductance Modulation of Gold Thin Films by Huge Charge Injection via Electrochemical Gating,” *Phys. Rev. Lett.* **108**, 066807 (2012).
- [30] Lucian Covaci and Frank Marsiglio, “Proximity effect and Josephson current in clean strong/weak/strong superconducting trilayers,” *Phys. Rev. B* **73**, 014503 (2006).